

GANGYOU SUN<sup>1</sup>, YUANDI XIA<sup>2</sup>, QINRONG KANG<sup>2</sup>,  
WEIZHONG ZHANG<sup>2\*</sup>, QINGZHEN HU<sup>2</sup>, WEI YUAN<sup>2</sup>

### APPLICATION OF BLSS-PE MINE 3D LASER SCANNING MEASUREMENT SYSTEM IN STABILITY ANALYSIS OF A URANIUM MINE GOAF

Accurate understanding of the three-dimensional (3D) morphology of a complex goaf and its relative displacement in space is a precondition to further analyzing the stability of the cavity. In this study, to make an accurate stability analysis of the goaf, laser detection and numerical simulation are used to study the interior space form of goaf and the change characteristics of stress and displacement in goaf. The results of the study show that the BLSS-PE mining 3D laser system as a field detection tool can detect the morphology of the cavity more comprehensively and improve the accuracy of the detection data to a certain extent. Combined with the numerical simulation software analysis, it can be seen that the maximum principal stress in the 818-2# goaf increases after excavation. In addition, the maximum value appears in the top and bottom plates of the goaf, and the minimum stress remains nearly unchanged. The tensile stress appears in the upper and lower plates but is lower than the surrounding rock. The maximum horizontal and vertical displacements of the 818-2# goaf are small. The plastic zone appears in the surrounding rock of the goaf as the mining work progresses, but the area is small. It is concluded that the goaf is relatively stable overall. The research results may provide a strong reference for ground pressure management in mines and comprehensive control of goaves.

**Keywords:** 3D laser; goaf; stability

## 1. Introduction

As the intensity of mining increases, a large amount of ore is extracted leading to the formation of a complex goaf. In addition, the original stress balance is broken, and the overlying rock layer is deformed owing to the loss of support, resulting in the collapse of the extraction goaf

<sup>1</sup> THE FOURTH RESEARCH AND DESIGN ENGINEERING CORPORATION, CHINA

<sup>2</sup> SCHOOL OF RESOURCES AND SAFETY ENGINEERING, WUHAN INSTITUTE OF TECHNOLOGY, CHINA

\* Corresponding author: [wzzhang1120@126.com](mailto:wzzhang1120@126.com)



© 2023. The Author(s). This is an open-access article distributed under the terms of the Creative Commons Attribution-NonCommercial License (CC BY-NC 4.0, <https://creativecommons.org/licenses/by-nc/4.0/deed.en>) which permits the use, redistribution of the material in any medium or format, transforming and building upon the material, provided that the article is properly cited, the use is noncommercial, and no modifications or adaptations are made.

and sinking of the ground surface [1]. As the mine continues to expand deeper, the stability of the rock layers gradually decreases, resulting in the gradual deterioration of the mine's surrounding rock. Post-mining worksite conditions, in a strong and complex, and diverse surrounding rock ground pressure environment can easily cause the collapse of the mine roof and other accidents. Therefore, stability analysis of a goaf is important in the current mine production.

Studies have been conducted on the stability analysis of goaves to ensure sustainable development and safe operation of mines [2-5]. Accurate detection of the goaf is the premise of stability analysis and treatment of goaf. The main methods used in the area of cavity detection include the high-density resistivity method [6], seismic image method [7], ground-penetrating radar method [8], transient Rayleigh wave method [9] and laser three-dimensional scanning method [10]. With the increasing complexity and number of goaf, the requirements of engineers for detection accuracy have gradually increased, and the results obtained by geophysical exploration means cannot have a substantial effect on the treatment of mined areas. Therefore, the accurate detection technology represented by 3D laser scanning is widely used in the detection of the goaf because of its high efficiency. For example, Dong Longbin et al [11] used the C-ALS, a goaf detection system, to accurately detect the morphology of the goaf in the Yamansu underground mine and established a visualized 3D realistic model of the goaf, obtaining a more accurate 3D morphology of the goaf.

The main methods used in the early stage include the fuzzy mathematical method [12,13], Bayes discriminant method [14], vector analysis method [15], finite element method [16], and other mathematical methods. With the rapid development and wide application of numerical simulation technology in the fields of mining and geotechnical engineering, numerical analysis has been extensively employed. For example, Xiaoqing He et al. [17] used the KT9 ore body goaf of the Shuangwang gold mine as the research background to solve the stability problem. FLAC<sup>3D</sup> was employed as a technical platform to systematically analyze the changes in the rock stress field and displacement field around the goaf to clarify the stability of the goaf, which provided a theoretical basis for later pillar re-mining and goaf treatment. They solved the stability problem of the cavity, thus broadening the application of numerical simulation. However, this numerical analysis was limited to the stability analysis of the goaf under a single condition. Therefore, extensive research has also been conducted to investigate the stability change of the cavity under a coupling effect of multiple fields. With increasing emphasis on safety, the accuracy requirements for the stability analysis of the cavity have also increased, but the traditional numerical analysis of the stability of the cavity is based on a specific range determination, and the boundary of the goaf is considered regular [18-24]. This is inconsistent with the actual situation of goaf space.

Therefore, in order to solve the problem of inconsistency between the measured and designed space of the goaf and improve the accuracy of the stability analysis of the goaf. In this paper, we considered the 818-2# goaf of a uranium mine in Ganzhou, China National Nuclear Corporation as the research object. We adopted the BLSS-PE 3D laser goaf measurement system to survey the complex goaf at bidirectional according to the characteristics of uranium goaf and constructed a 3D solid model by using DIMINE software. Subsequently, we established a 3D model of the goaf with FLAC<sup>3D</sup> to obtain the numerical analysis model of the goaf based on the actual measurements. After the numerical simulation, the changes in the stress field and displacement field were obtained, and the stability influence of the mining void on the surrounding rocks was analyzed. Consequently, the problem of inconsistency between the measured and designed spaces was solved, and a new method for analyzing the stability of the mining void in complex mines was proposed.

## 2. Project Summary

The kt-818-2 ore body is located in section 710#, striking nearly east-west, and approximately 40 m long. It has an average thickness of 5 m and a deposition height of 166-200 m, tilting south and dipping to the north at a dip angle of approximately  $72^\circ$ . The ore body is composed of medium-grained dolomite granite and medium-grained small porphyritic black mica granite. The surrounding rocks of the ore body are more stable; the protodyakonov number of the rock ore is 5-11; the natural repose angle of the rock is  $37^\circ$ ; the weight of the ore is  $26000 \text{ t/m}^3$ , and the loosening coefficient of the ore is 1.65. The ore body has no obvious boundary with the surrounding rocks and is in a gradual relationship. According to the normal recovery schedule, the quarry should be finished in 9 months. However, during the recovery process, it was found that the mineralization in the middle section of 200 m is better, and if the top pillar is left for recovery, the amount of loss in the later period is larger. To maximally recover the metal and avoid waste, the uranium ore was recovered to 194 m elevation in the later period, and then continued to be mined up 16 m and recovered to the middle section of 200 m to 210 m elevation, which significantly recovered the metal.

## 3. Construction of Three-dimensional Goaf Model

### 3.1. BLSS-PE 3D laser scanning measurement system

BLSS-PE mining 3D laser scanning measurement system is developed by Beijing General Research Institute of Mining and Metallurgy, specifically for China's mining application conditions and needs (see Fig. 1), with its miniaturized scanning master, wireless transmission system, high protection system, adaptive spatial resolution optimization technology, blind area identification technology, multi-station splicing technology, no total station coordinate transfer technology to provide mines with fast, high-precision non-contact three-dimensional space rapid measurement. The laser scanner's technical parameters are shown in TABLE 1.



Fig. 1. Measurement system

TABLE 1

The technical parameters of the laser scanner

Scanner	Accuracy of ranging @ distance	Measurement range /m	Scan rate / (Point / second)	Spot size @ distance	Horizontal	Vertical
BLSS-PE	4 mm @ 50	350 m	maximum 10000	9 mm @ 50 mm	360	360

### 3.2. Collection of primary data in goaf

The primary detection data of the goaf was collected using the BLSS-PE measurement system. In the field detection of the goaf, to avoid the limitations caused by the mine measurement points and instruments, the roadway near the measurement point was measured by vertical and horizontal scanning during the detection process to achieve accurate positioning of the location pattern of the underground space in the measured goaf using the roadway coordinates. The specific detection process is as follows:

- (1) Commissioning the System: Attached the scanning master to the extension pole or tripod adapter and connected the power supply to the power cord of the scanning mainframe; Pressing the power switch of the generator and establishing wireless communication between the scanning control terminal and the power pack. Finally opened the BLSS-PE measurement system software on the scanning control terminal to initialize the scanning host and set the scanning parameters to the system software.
- (2) Starting detection: Two measurement points, 818-2 E1-28 west and 818-2 E1-32 east, were selected for detection. for one quick scan by BLSS-PE measurement system software; refinement of scanning parameters based on the quick scan results and the start of the scan.
- (3) Checking the results: Monitored the scanning process in real-time via the software interface and confirmed that the BLSS-PE has completed the scan as expected and stopped scanning. Results and data were checked after the detection is finished.

### 3.3. Pre-processing of primary measurement data

The BLSS-PE 3D laser scanning measurement system was used to scan the 818-2# goaf. Thereafter, we obtained the point cloud data of the spatial morphology position of the goaf, imported the point cloud file into the BLSS-PE measurement system, and generated the “.blss” point cloud file. In the 3D visualization environment, the spatial pattern of the goaf and the nearby roadway is presented. After using the 3D laser scanning system to complete the detection and processing of the goaf’s spatial morphology data, before the cavity model’s construction, other necessary data analysis processing must be performed on the obtained point cloud data, which is carried out as follows:

- (1) Data filtering: The data obtained after the detection of the goaf may be inaccurate owing to the external factors and impact of the environment of the cavity itself, resulting in invalid points in the measured data; therefore, to ensure the accuracy of the data after detection, the data is usually filtered first.
- (2) Splicing of data: Owing to the blocking effect of the ore or ore pillar in the cavity, the point cloud data obtained may not restore the real spatial shape to some extent. For

the characteristics of the cavity, the multi-point detection method is used to detect it, and then the 3D point cloud data are stitched together by establishing the coordinate system.

- (3) Data fitting: The point cloud data obtained after vertical and horizontal scanning are fitted to the goaf solid model to make the final point cloud file a more realistic reflection of the spatial shape of the cavity(see Fig. 2), and only when the cavity point cloud file completes the data pre-processing, the construction of the three-dimensional model of the underground goaf begins.

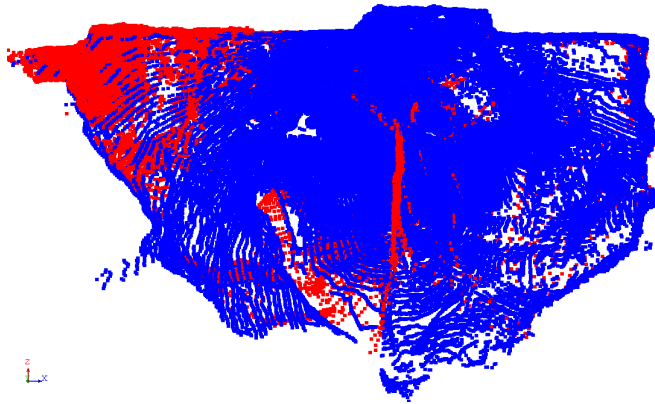


Fig. 2. Main view of the point cloud data of the 818-2# quarry goaf

### 3.4. 3D goaf solid model construction

After converting the point cloud data into a format that can be imported into the DIMINE software, the solid modeling function in the DIMINE software is used to construct the 3D graphic outline of the goaf to realize its 3D visualization. The measured 3D model of the 818-2 # cavity is shown in Fig. 3.

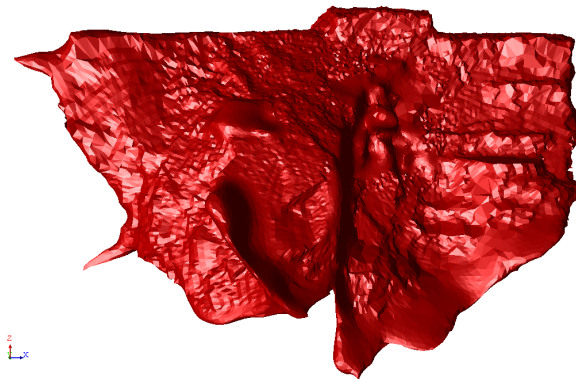


Fig. 3. 818-2# quarry goaf solid model fitting diagram

## 4. Construction of the numerical model

### 4.1. Selection of the constitutive model

When constructing a numerical model, the mechanical properties of the material should be defined. Therefore, the choice of the constitutive model is a prerequisite for the correct definition of material properties. According to the characteristics of the studied materials, the Mohr-Coulomb criterion is used for all numerical analyses, i.e., the elastic-plastic model is used in the static and dynamic calculations. The mechanical model is as follows:

$$\frac{\sigma_1 - \sigma_3}{2} = \frac{\sigma_1 + \sigma_3}{2} \sin \varphi + C \cos \varphi \quad (1)$$

$$f_s = \sigma_1 - \sigma_3 \frac{1 + \sin \varphi}{1 - \sin \varphi} - 2C \sqrt{\frac{1 + \sin \varphi}{1 - \sin \varphi}} \quad (2)$$

$\sigma_1, \sigma_3$  — the maximum and minimum principal stresses;

$C, \varphi$  — the material cohesion and internal friction angle;

$f_s$  — the damage judgment coefficient;

When  $f_s \geq 0$ , the material is in a plastic flow state. When  $f_s \leq 0$ , the material is in the elastic deformation stage. In the tensile stress state, if the tensile stress exceeds the tensile strength of the material, the material will undergo tensile failure.

### 4.2. Physical and mechanical parameters and boundary conditions of the surrounding rock

According to the characteristics of this deposit, the ore body and surrounding rock were selected as the main mechanical media for analysis in this study. The strength parameters of this calculation were discounted according to the commonly used criteria for discounting the strength parameters of rock bodies, with the angle of internal friction  $\varphi$  discounted by 0.85, cohesion discounted by 1/7-1/10, and modulus of elasticity discounted by 2/3. The strength mechanical parameters of the uranium ore rock body are obtained as shown in TABLE 2.

The bulk and shear moduli were used in the FLAC<sup>3D</sup> model calculations to characterize the elastic modulus and Poisson's ratio [25]. Therefore, the conversion between the functions was performed by applying Equation 3 before performing the analysis.

$$\left. \begin{aligned} K &= \frac{E}{3(1-2\mu)} \\ G &= \frac{E}{2(1+\mu)} \end{aligned} \right\} \quad (3)$$

$K$  — Bulk modulus;

$G$  — Shear modulus;

$E$  — elastic modulus;

$\mu$  — Poisson's ratio.

TABLE 2

Mechanical parameters of rock mass of uranium mine

Quality	Uniaxial compression resistance (MPa)	Bulk modulus (GPa)	Shear modulus (GPa)	Poisson's ratio	volumetric weight (MN/m <sup>3</sup> )	Tensile strength (MPa)	Internal friction angle (°)	Internal cohesion (MPa)
Orebody	110	2.86	1.82	0.24	0.026	3	30	3
Surrounding Rock	110	2.86	1.82	0.24	0.026	3	30	3

Initial stress: Owing to the lack of mines without initial stress tests, the initial stress in this study was calculated using the rock gravity stress.

Calculation of boundary conditions: Displacement boundary conditions were used, i.e., displacement constraints were imposed on the surface of the model, and the stress converted from the weight of the upper rock mass was applied at the upper boundary. According to the 3D models of the surface and cavity, it is known that the surface is approximately 30 m away from the upper boundary of the numerical model 270 horizontal distance, and the stress applied at the upper boundary is 0.9 MPa.

### 4.3. Numerical Analysis Model

The “DIMINE to FLAC<sup>3D</sup>” data conversion program was used to convert the centroid file of the uranium mine cavity model into a FLAC<sup>3D</sup> grid data file. The detailed steps of the cavity modeling are as follows:

- (1) DIMINE is employed to build the surface model, rock model, and cavity model within the required range for the numerical simulation of the cavity.
- (2) Based on the constraint of the solid model, the block model of the computational domain is constructed.
- (3) Export block unit centroid file.
- (4) Convert centroid file to FLAC<sup>3D</sup> grid data files using the “DIMINE to FLAC<sup>3D</sup>” data conversion program.
- (5) Numerical calculation model generation using FLAC<sup>3D</sup> grid data files, and finally, a FLAC<sup>3D</sup> numerical calculation model of the uranium mine mine-out area is established, generating a total of 531,441 network nodes and 512,000 units, as shown in Fig. 4.

## 5. Numerical Simulation Results and Analysis

### 5.1. Stress Analysis

#### (1) X-profile analysis

Figs. 5(a) and 5(b) show the maximum principal stress distribution in the surrounding rock before and after the mine excavation on the X-profile of the 818-2# quarry. Figs. 6(a) and 6(b) show the minimum principal stress distribution in the surrounding rock before and after the mine excavation on the X-profile of the 818-2# quarry.

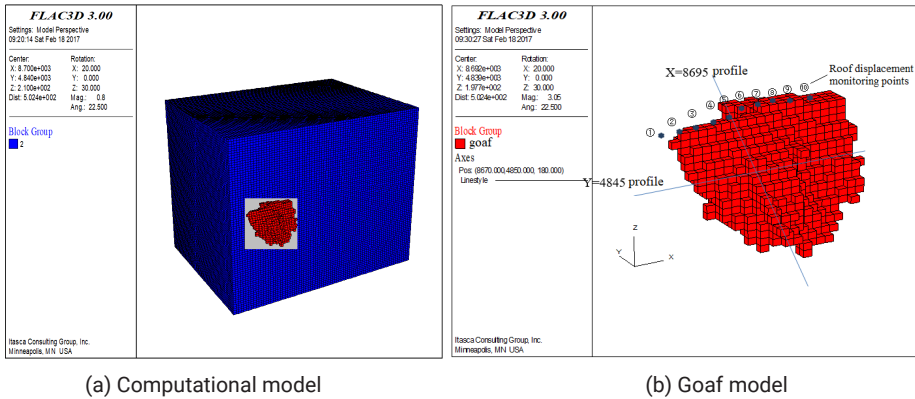
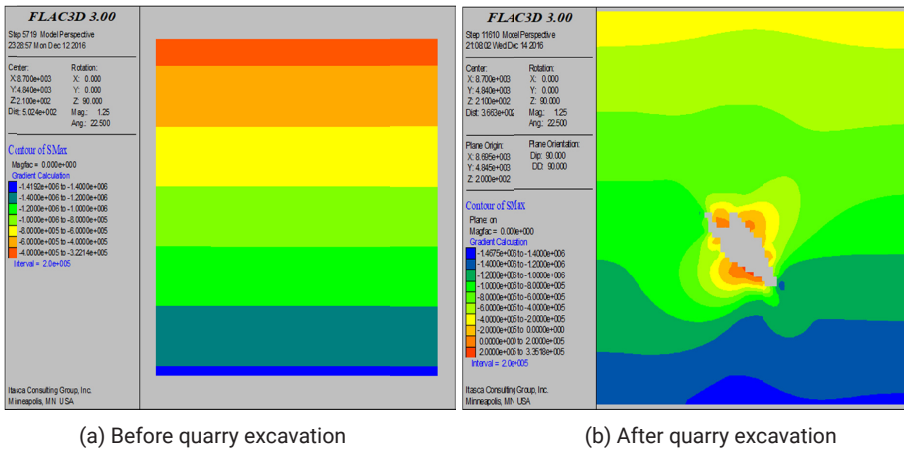
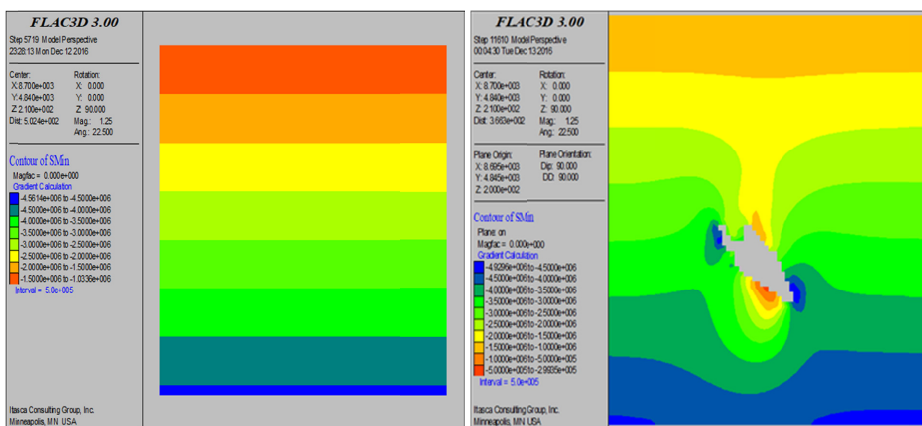
Fig. 4. 818-2# FLAC<sup>3D</sup> numerical calculation model of goaf

Fig. 5. 818-2# Maximum principal stress distribution before and after quarry excavation

From Fig. 6(b), it can be observed that the minimum principal stress changes and tends to increase after the excavation of the quarry. According to the principal stress distribution diagram before and after excavation, the minimum principal stress increases from 4.5 to 4.9 MPa after excavation, and the maximum value appears at the top and bottom plates of the goaf. The minimum principal stress typically remains unchanged, with a maximum value of 1.4 MPa. With the excavation of the quarry, tensile stress appears at the top and bottom plate positions, and the stress value is 0.5 MPa. According to TABLE 2, the tensile strength of the surrounding rock is 3 MPa. Therefore, in the tensile stress state, the tensile strength does not exceed its tensile strength, and the surrounding rock of the goaf remains stable.

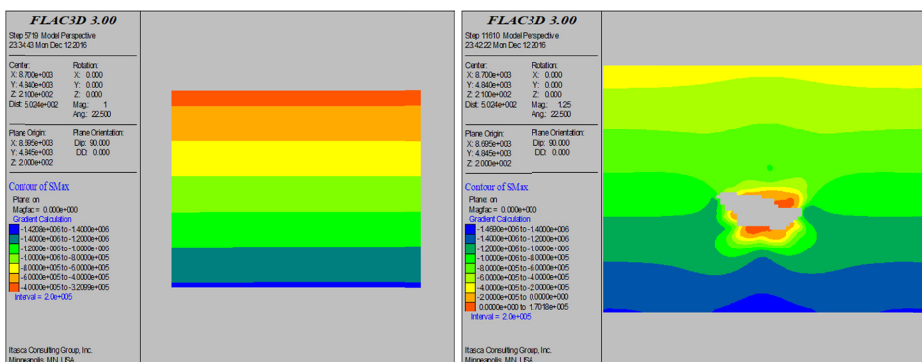
## (2) Y-profile analysis

Figs. 7(a) and 7(b) show the maximum principal stress distribution in the surrounding rock before and after the excavation on the Y-profile of 818-2# quarry. Figs. 8(a) and 8(b) show the



(a) Before quarry excavation (b) After quarry excavation

Fig. 6. 818-2# Minimum principal stress distribution before and after quarry excavation

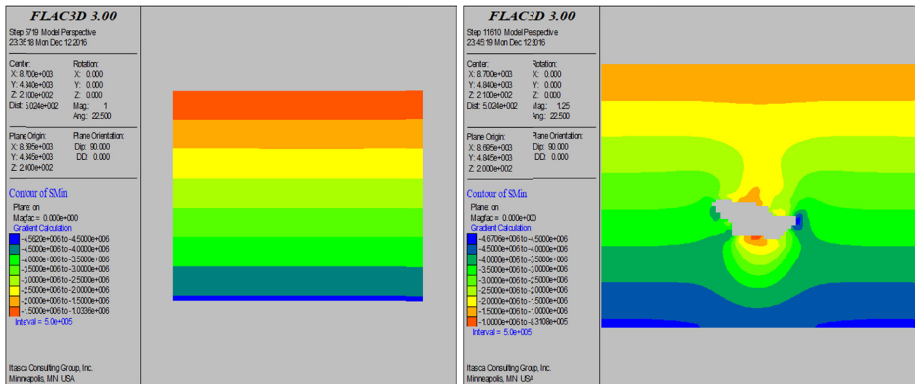


(a) Before quarry excavation (b) After quarry excavation

Fig. 7. 818-2# Maximum principal stress distribution before and after quarry excavation

minimum principal stress distribution in the surrounding rock before and after the excavation on the Y-profile of 818-2# quarry.

As can be observed from the figures, the maximum principal stress changed more noticeably after the excavation of the quarry, and its value showed a trend of gradual increase. According to the principal stress distribution before and after excavation, the minimum principal stress increased from 4.56 MPa to 4.67 MPa after excavation. The maximum value appeared at the top and bottom plates of the goaf. The maximum principal stress remains unchanged, with a maximum value of 1.4 MPa. With the excavation of the quarry, tensile stress appears at the top and bottom plate positions, and the stress value is 0.17 MPa, which is lower than the tensile strength of the surrounding rock. Therefore, the surrounding rock in the goaf is stable.



(a) Before quarry excavation

(b) After quarry excavation

Fig. 8. 818-2# Minimum principal stress distribution before and after quarry excavation

## 5.2. Displacement Analysis

Owing to the excavation of the cavity, the stresses and displacements in the surrounding rock change. In the analysis of the stability of the surrounding rock, we focused on the characteristics of the distribution changes of stress and displacement. The changes of displacement can reflect the stability state of the surrounding rock more directly than the stress changes. Figs. 9 and 10 present the horizontal and vertical displacement distribution changes after the formation of the cavity in the X-profile and Y-profile, respectively; it can be observed that the change of the displacement distribution of the surrounding rock presents the following characteristics.

- 1) After back mining 818-2# quarry, the maximum horizontal displacement occurs in the quarry's upper side and lower plate near the roof and floor plate position.
- 2) After the 818-2# quarry was retrieved, the maximum vertical displacement appeared at the roof and floor plate of the quarry.
- 3) The maximum vertical displacement is larger than the maximum horizontal displacement, which is vertically consistent with the direction of the maximum main stress in the mine.
- 4) After the formation of the cavity, the maximum displacement of the roof and floor plates of the cavity and the displacement of two ribs is approximately 10 mm, and the cavity is in a stable state.

### (3) Analysis of roof displacement in goaf

By setting up monitoring points on the roof of the goaf (see Fig. 4(b)), the process of displacement of the roof is monitored throughout the calculation process.

Fig. 11 shows the final displacement diagram of the roof monitoring points. As can be observed from the figure, the maximum displacement occurs near monitoring point 6. After the formation of the goaf, the roof plate drops rapidly and then tends to stabilize, indicating that the roof plate is in a stable state after the formation of the goaf.

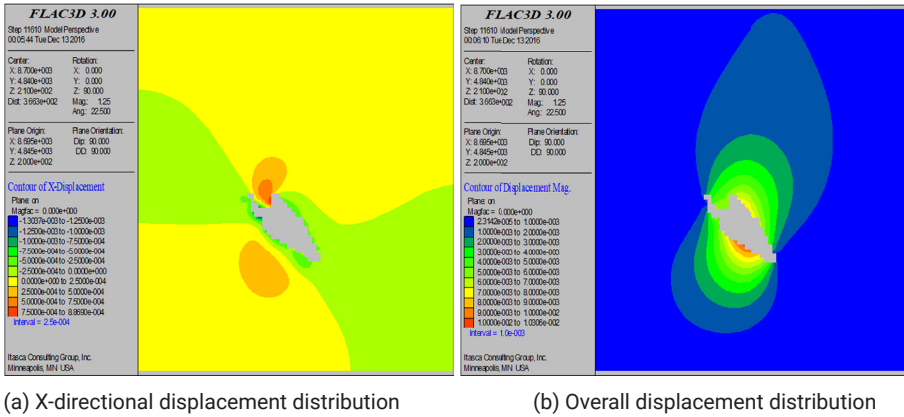


Fig. 9. 818-2# Displacement distribution map after quarry excavation

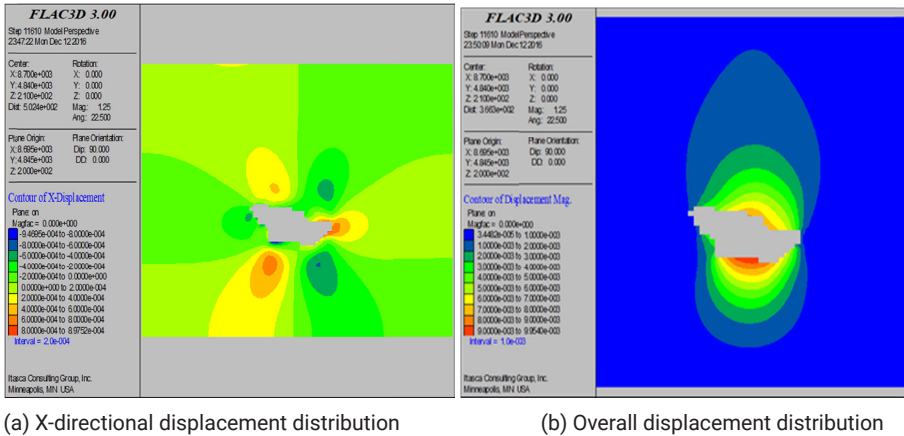


Fig. 10. 818-2# Displacement distribution map after quarry excavation

### 5.3. Plastic Zone Analysis

Fig. 12(a) shows the distribution of the plastic zone of the surrounding rocks in the X-profile after the formation of the cavity. It can be observed that with the gradual recovery of the quarry, the plastic zone appears in some areas of the surrounding rocks in the cavity; specifically, in the upper position of the lower plate of the quarry, the area of the plastic zone is small and has a slight influence on the stability of the entire cavity. The cavity is in a stable state overall.

Fig. 12(b) shows the distribution of the plastic zone of the surrounding rocks in the Y-profile after the formation of the cavity. It can be observed in the figure that with the gradual recovery of the quarry, the plastic zone appears in some areas of the surrounding rocks in the cavity. In particular, in the top plate of the quarry and the eastern location of the quarry, the area of the plastic zone is significantly small and has a slight influence on the stability of the goaf. The goaf is in a stable state overall.

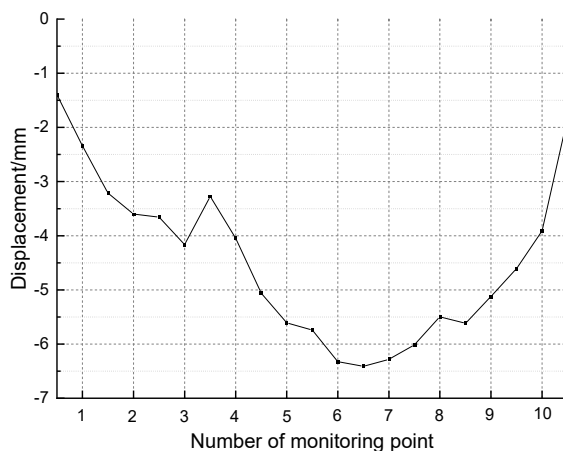
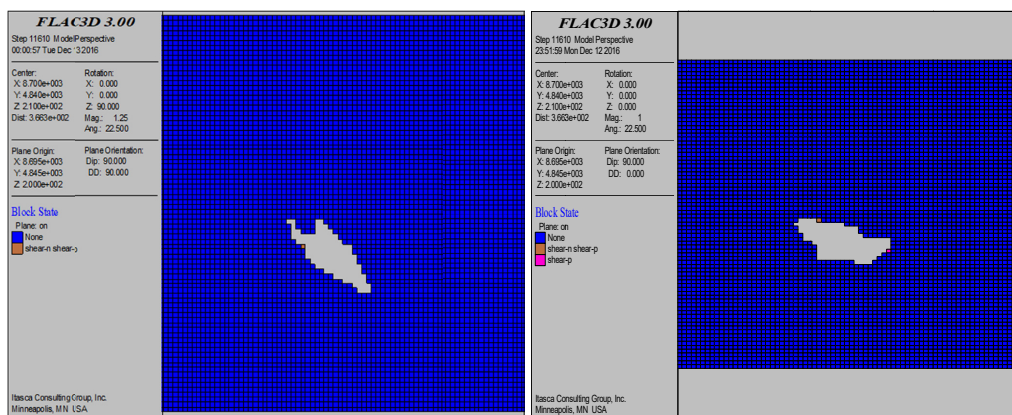


Fig. 11. Displacement map of roof monitoring points



(a) X-profile

(b) Y-profile

Fig. 12. Distribution of plastic zone of surrounding rocks in the cavity after quarry excavation

## 6. Conclusions

- (1) When using 3D laser scanning technology to measure the spatial pattern of goaf, non-contact measurements can be achieved compared to traditional methods. As a result, the safety of the surveyor can be greatly ensured without compromising the accuracy of the measurement data. In addition, 3D laser scanning technology is a breakthrough in single-point measurement and enables the acquisition of large amounts of point cloud data of scanned objects at high density and resolution, with detailed descriptions of the target and high sampling rates. It can improve the accuracy of cavity detection and restore the true shape of the goaf. By employing BLSS-PE 3D laser scanning and measuring system to detect the goaf and constructing the 3D model of the goaf by min-

ing software DIMINE, we realized a 3D solid model of the goaf of 818-2# quarry that can accurately detect the 3D form of the goaf.

- (2) The article presents a comprehensive analysis of the stability of the cavity through 3D laser field detection combined with numerical simulations and empirical formulas. The BLSS-PE 3D laser scanning and measurement system are used as a means of airspace detection, which greatly ensures the safety of the measurement personnel without compromising the accuracy of the measurement data. Three-dimensional laser detection technology will become the future development trend of airspace detection.
- (3) According to the constructed 3D model of the goaf using FLAC<sup>3D</sup> for numerical calculation, the coupling of the actual measurement technology of the goaf with the numerical simulation technology was realized. According to the simulation results, the influence of the goaf on the stability of the surrounding rock was analyzed. From the analysis of stress change characteristics, displacement change characteristics, and plastic zone change characteristics, the 818-2# goaf was in a stable state; however, for mine safety considerations, the goaf should be treated promptly. The results of the study show that the 3D laser detection technology can enhance the scientific analysis of the stability of the cavity and has good application value.
- (4) As 3D laser scanning needs to be developed on a more stable working platform, but the geological environment of the mine is complex, the actual work will be affected to some extent. From the point cloud fitting diagram, it can be seen that the uneven distribution of the point cloud data has led to difficulties in synthesising the solid model at the corners. The accuracy of the results can be increased in the future by scanning multiple points from different boreholes into the goaf.

### Data Availability

The data used to support the findings of this study are included within the article.

### Conflicts of Interest

The author(s) declare(s) that there is no conflict of interest regarding the publication of this paper.

### Funding Statement

This project is funded by the National Natural Science Foundation of China(52174086)

### References

- [1] Y.H. Huang, L. Wen, M. Huang, H.S. He, Y. Pan, J.L. Shen, Research on Fuzzy Evaluation System for Stability of Complex Goaf in Metal Mine. *Mining Research and Development* **39** (12), 63-67 (2019). DOI: <https://doi.org/10.13827/j.cnki.kyyk.2019.12.012>
- [2] Q.Y. Ren, Stability analysis of goaf based on DIMINE-MIDAS/GTS. *Nonferrous Metals (Mining-Part)* **72** (05), 55-61 (2020).
- [3] H.H. Jia, Stability Analysis of Goaf Based on C-ALS Data Point Cloud and FLAC3D Coupled Modeling. *Journal of Water Resources and Architectural Engineering* **261** (06), 672-1144 (2021).

- [4] G.F. Chen, C.F. Luo, L.X. Zhong, F. Chen, Stability analysis and treatment plan selection of goaf based on RHINO-FLAC-(3D). *Mining Research and Development* **39** (09), 30-35 (2019).
- [5] Z.P. Zhang, F. Li, H.C. Zhang, Stability analysis of goaf in steeply inclined thick coal seam and evaluation of grouting treatment effect. *Science Technology and Engineering* **21** (04), 1312-1317 (2021).
- [6] Y. Mou, W.W. Li, W.F. Gao, Experimental study on distributed high-density electrical method to detect shallow buried deep mining areas. *Coal Engineering* **51** (09), 152-157 (2019).
- [7] J.P. Liu, Y.Y. Wang, Z. Liu, X.K. Pan, Y.Q. Zong, Advances and applications of near-surface reflection and refraction methods. *Journal of Geophysics* **5** (09), 3286-3305 (2015).
- [8] G.Q. Xue, D.M. Pan, J.C. Yu, A review of geophysical exploration applications in coal mining areas. *Advances in Geophysics* **33** (05), 2187-2192 (2018).
- [9] F.Z. Zhai, P.F. Xu, L.N. Pan, B. Chen, C.J. Zhang, S.Q. Ling, Research on physical prospecting methods for concealed hillside survey of Ningbo rail transit. *Advances in Geophysics* **32** (04), 1856-1861 (2017).
- [10] W.Z. Yu, Y.G. Wang, S.Z. Zhou, Research on 3D modeling and application technology based on laser point cloud data. *Mechanical Design* **38** (09), 118-119 (2021). DOI: <https://doi.org/10.13841/j.cnki.jxsj.2021.09.037.2021>
- [11] L.B. Dong, S.Q. Wang, S.Y. Lin, S. Pang, H.B. Qiao, Application of C-ALS-based 3D laser scanning technology in the detection of mining areas. *Nonferrous Metals (Mining part)* **71** (02), 1-4 (2019).
- [12] H.J. Wang, X.D. Bian, X.W. Deng, N.Q. Feng, Lu Bangsteady, Evaluation of the suitability of underground space development and utilization in coal mines based on fuzzy mathematical theory – Baiyuan coal mine as an example. *Northwest Geology* **54** (04), 156-170 (2021).
- [13] Razak Karim, Ganda M. Simangunsong, Budi Sulistianto, Arnol Lopulalan, Stability analysis of paste fill as stope wall using analytical method and numerical modeling in the Kencana underground gold mining with long hole stope method. *Procedia Earth and Planetary Science* **6**, 474-484 (2013).
- [14] F.Q. Gong, K.W. Liu, Z.G. Li, Bayes discriminant analysis method for predicting the risk of mining collapse. *Journal of Mining and Safety Engineering* **7** (01), 30-34+39 (2010).
- [15] Y.Z. Liu, S.H. Pan, X.Q. Chen, X.T. Zou, Q. Zhang, B.T. Zhang, Stability analysis of the top and bottom rib in the open pit in the underground mining of Huogezhuang South Mine Section. *Mining and Metallurgy Engineering* **35** (06), 25-29 (2015).
- [16] J.Y. Deng, H.G. Pan, C. Lin, Ground stability and governance method of coal mine goaf based on ANSYS. *Coal Technology* **32** (10), 159-161 (2013).
- [17] X.Q. He, T.H. Ling, F. Cao, Research on stability analysis and treatment of goaf based on FLAC~(3D). *Mining Research and Development* **36** (09), 34-37 (2016).
- [18] Z.Q. Luo, C.Y. Xie, J.M. Zhou, Numerical analysis of stability for goaf in multi-field coupling. *Journal of Central South University* **22** (02), 669-675 (2015.)
- [19] X.M. Liu, Z.Q. Luo, C.X. Yang, B. Zhang, H. Lu, Numerical simulation analysis of the stability of goaf based on real measurements. *Geotechnics* **28** (S1), 521-526 (2007).
- [20] M. Huang, S.H. Tang, Y.H. Huang, Y.B. Wu, Numerical simulation study on stability analysis of goaf based on ANSYS-FLAC~(3D). *Mining Research and Development* **37** (06), 78-83 (2017).
- [21] W.D. Song, J.X. Fu, J.H. Du, C.L. Zhang, Stability analysis of metal mining goaf cluster based on precision detection. *Geotechnics* **33** (12), 3781-3787 (2012).
- [22] K.W. Liu, Laser three-dimensional detection and visualization of open-pit mining goaf and its stability analysis. *Zhongnan University* (2012).
- [23] H. Tang, Z.G. He, H.B. Lian, Numerical Simulation Analysis on Stability of Coal Pillar of Empty Mine Goaf in North of Shanxi Province. *Applied Mechanics and Materials* **470** (2013).
- [24] Tümay Kadakci Koca, A Conceptual Sector-Scale Numerical Modeling of a Landslide in an Open Pit Mine. *Archives of Mining Sciences* **67** (02), 275-287 (2022). DOI: <https://doi.org/10.24425/ams.2022.141458>
- [25] T. Janoszek, The Assessment of Longwall Working Stability Based on the Mohr-Coulomb Stress Criterion – Numerical Analysis. *Archives of Mining Sciences* **65** (03), 493-509 (2020). DOI: <https://doi.org/10.24425/ams.2020.134131>